Three-dimensional structure of the 3'X-tail of hepatitis C virus RNA in monomeric and dimeric states

Ángel Cantero-Camacho, Lixin Fan, Yun-Xing Wang and José Gallego

SUPPLEMENTARY MATERIAL

SUPPLEMENTAL FIGURE LEGENDS

Figure S1. RNA sequences studied by SAXS. The self-complementary DLS nucleotides are highlighted in red.

Figure S2. Electrophoretic and chromatographic analysis of DLS-containing SL2' and 3'X sequences. (A) Native gel electrophoresis of sequence SL2', previously folded in 10 mM Tris-NaCl (pH 7.0) and 0.1 mM EDTA, with no added salts or additionally containing 2 mM $MgCl_2$. (B) Size exclusion chromatography of sequence 3'X, previously folded in 10 mM Tris-NaCl (pH 7.0), 0.1 mM EDTA, 2 mM $MgCl_2$ and 50mM NaCl. The buffer running through the column was identical. These solution conditions facilitated the isolation of homogeneous 3'X dimer samples. Conditions for (A): 31 μM SL2', 8% polyacrylamide, 89 mM Tris-Borate (TB) running buffer. The experiment was run for 60 minutes at 4 ^{o}C and 150 V.

Figure S3. Kratky plots of subdomains SL1 (A) and SL2' (B) and full-length domain 3'X (C) at low (red) and higher (blue) ionic strength.

Figure S4. Flexibility analysis of subdomain SL2' at low ionic strength. (A) Average *ab-initio* envelope of SL2' at low ionic strength, superposed with the best energy-minimized atomic model (blue), and with the same model after flexible refinement with SREFLEX(Panjkovich and Svergun 2016) and energy-minimization (black). (B) Experimental SAXS curve of subdomain SL2' at low

ionic strength (black dots), overlaid with the theoretical profiles calculated from the best energy-minimized model before (blue line) and after (red line) flexibility refinement with SREFLEX. The χ^2 values were 8.58 and 2.04, respectively.

Figure S5. Evaluation of atomic models of HCV domain 3'X containing three double-helical stems. (A) Secondary structure of domain 3'X containing three stems (SL1, SL2 and SL3). This structure was not detected by NMR spectroscopy at the different ionic strength solution conditions tested. (B) Experimental SAXS envelope of domain 3'X obtained under low ionic strength, superposed with the best energy-minimized atomic model generated with theoretical three-stem (SL1, SL2 and SL3) secondary structure restraints, selected by fitting the theoretical SAXS profiles to the experimental curve. (C) Experimental low-salt SAXS profile of domain 3'X (black dots), overlaid with the theoretical profiles calculated from the best three-stem (red line) and two-stem (blue) energy-minimized atomic models. The χ^2 values were 1.46 and 0.66, respectively. Theoretical profile calculations with MultiFoXS(Schneidman-Duhovny et al. 2016) using mixtures of two-stem and three-stem atomic models indicated a 100% presence of the two-stem model.

Figure S6. Reconstruction of the structure of full-length domain 3'X with the shapes of individual subdomains SL1 and SL2' at low and higher ionic strength. (A) Superposition of the *ab-initio* envelope of full-length domain 3'X (light green) with those of subdomains SL2' (salmon) and SL1 (blue) under low ionic strength conditions (monomeric state). (B) Overlay of the shape of full-length domain 3'X (olive green) with those of subdomains SL2' (purple) and SL1 (blue) at higher salt concentration (dimeric form conditions). In (A) and (B), the superposed envelopes are shown in two different orientations.

SUPPLEMENTAL TABLES

Table S1. Theoretical and experimental molecular weights (MW) of full-length domain 3'X and subdomains SL1 and SL2' in conditions of low and higher ionic strength. The experimental values were calculated from the SAXS data using three different methods.

Sequence	**Ionic strength** $MgCl_2$/NaCl (mM)	**MW** theoretical (Da)	**MW** [a,b] experimental (Fischer et al. 2010)	**MW** [a] experimental (Rambo and Tainer 2013)	**MW** [a] experimental (Petoukhov et al. 2012)
3'X	0/0	31707	34145 (1.08)	32914 (1.04)	30463 (0.96)
3'X	2/50	63414	65511 (1.03)	64231 (1.01)	60855 (0.96)
SL1	0/0	14970	15272 (1.02)	16239 (1.08)	16045 (1.07)
SL1	2/0	14970	15605 (1.04)	15637 (1.04)	16045(1.07)
SL2'	0/0	17854	18758 (1.05)	18484 (1.04)	19523 (1.09)
SL2'	2/0	35707	36328 (1.02)	35201 (0.99)	30718 (0.86)

[a]Expressed in Da, with normalized values relative to theoretical molecular weights shown in parentheses

[b]Calculated using a maximum q value of 0.5 $Å^{-1}$.

Table S2. Monomer and dimer formation by domain 3'X and subdomain SL2' sequences, monitored by fitting the experimental scattering curves measured at low and higher ionic strength with the theoretical profiles obtained with the best energy-minimized monomer and dimer atomic models, and with a mixture of the best energy-minimized monomer and dimer models. FoXS was used for fitting single models (monomer or dimer), and MultiFoXS and MES were applied for fitting mixture models. The analyses focused on dimerization-capable 3'X and SL2' sequences containing the palindromic DLS tract.

Sequence	**Ionic strength** $MgCl_2$/NaCl (mM)	χ^2 (monomer atomic model)	χ^2 (dimer atomic model)	χ^2 (mixture of monomer and dimer)	**monomer/dimer content** (%)
3'X	0/0	0.66	9.42	0.37	93/7
3'X	2/50	722	19.99	19.99	0/100
SL2' [a]	0/0	2.04	21.72	1.42	92/8
SL2'	2/0	21.62	1.74	1.69	5/95

[a]The SL2' monomer model was obtained after exploring the conformational space with SREFLEX(Panjkovich and Svergun 2016). Before flexibility refinement, the χ^2 values were 8.58 for the monomer model, and 3.20 with 83% monomer content for the mixture of dimer and monomer models.

SUPPLEMENTAL REFERENCES

Fischer H, de Oliveira Neto M, Napolitano HB, Polikarpov I, Craievich AF. 2010. Determination of the molecular weight of proteins in solution from a single small-angle X-ray scattering measurement on a relative scale. *Journal of Applied Crystallography* **43**: 101-109.

Panjkovich A, Svergun DI. 2016. Deciphering conformational transitions of proteins by small angle X-ray scattering and normal mode analysis. *Physical Chemistry Chemical Physics* **18**: 5707-5719.

Petoukhov MV, Franke D, Shkumatov AV, Tria G, Kikhney AG, Gajda M, Gorba C, Mertens HDT, Konarev PV, Svergun DI. 2012. New developments in the ATSAS program package for small-angle scattering data analysis. *Journal of Applied Crystallography* **45**: 342-350.

Rambo RP, Tainer JA. 2013. Accurate assessment of mass, models and resolution by small-angle scattering. *Nature* **496**: 477-481.

Schneidman-Duhovny D, Hammel M, Tainer JA, Sali A. 2016. FoXS, FoXSDock and MultiFoXS: Single-state and multi-state structural modeling of proteins and their complexes based on SAXS profiles. *Nucleic Acids Res* **44**: W424-429.

3'X 5' GGUGGCUCCA UCUUAGCCCU AGUCACGGCU AGCUGUGAAA GGUCCGUGAG CCGCUUGACU GCAGAGAGUG CUGAUACUGG CCUCUCUGCA GAUCAAGU 3'

SL1 5' GCUUGACUGC AGAGAGUGCU GAUACUGGCC UCUCUGCAGA UCAAGU 3'

SL2' 5' GGUGGCUCCA UCUUAGCCCU AGUCACGGCU AGCUGUGAAA GGUCCGUGAG CCGCU 3'

,

Fig. S1

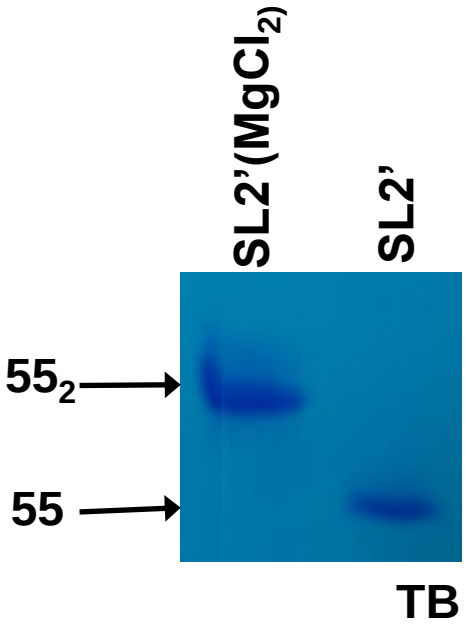
SL2'(MgCl2)
SL2'
55₂
55
TB

A

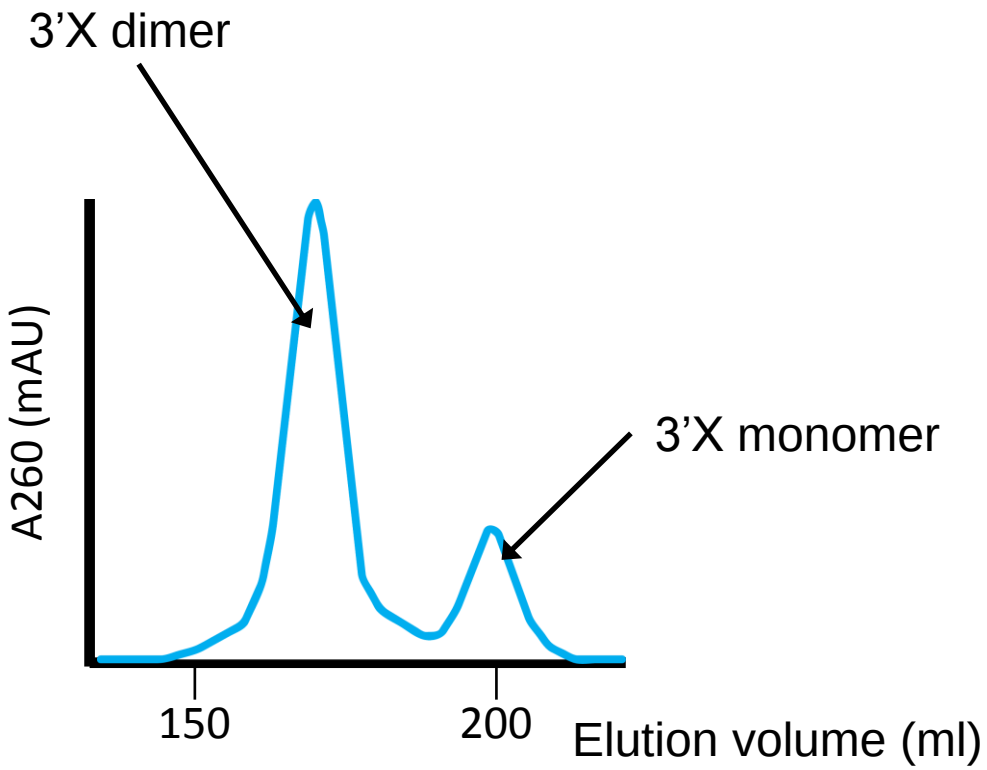
3'X dimer
3'X monomer
A260 (mAU)
150
200
Elution volume (ml)

B

Fig. S2

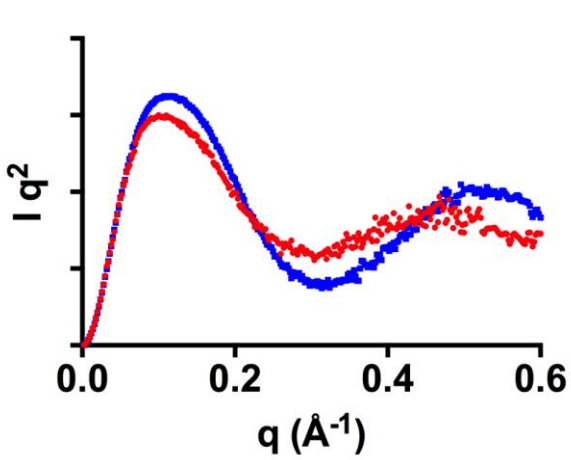

A

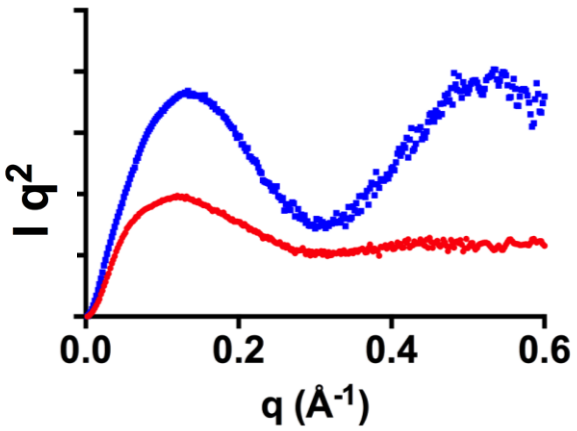

B

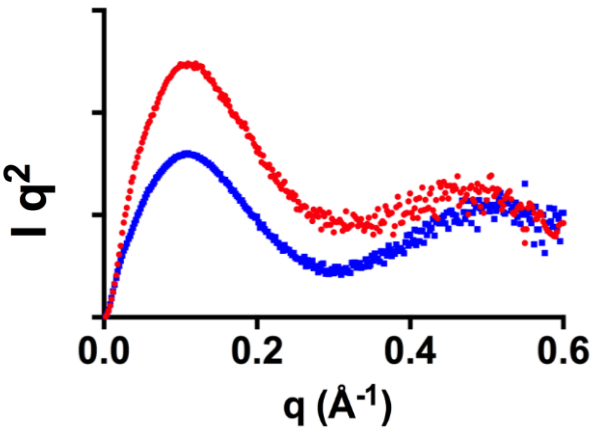

C

Fig. S3

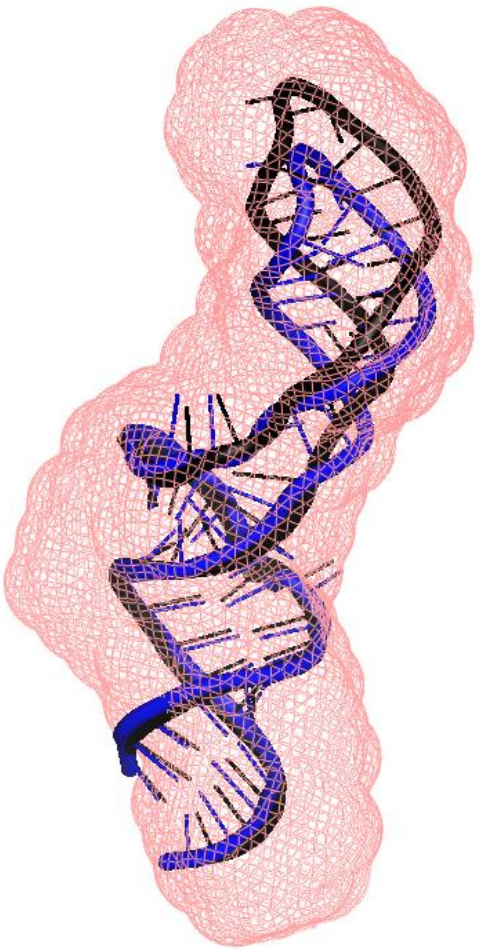

A

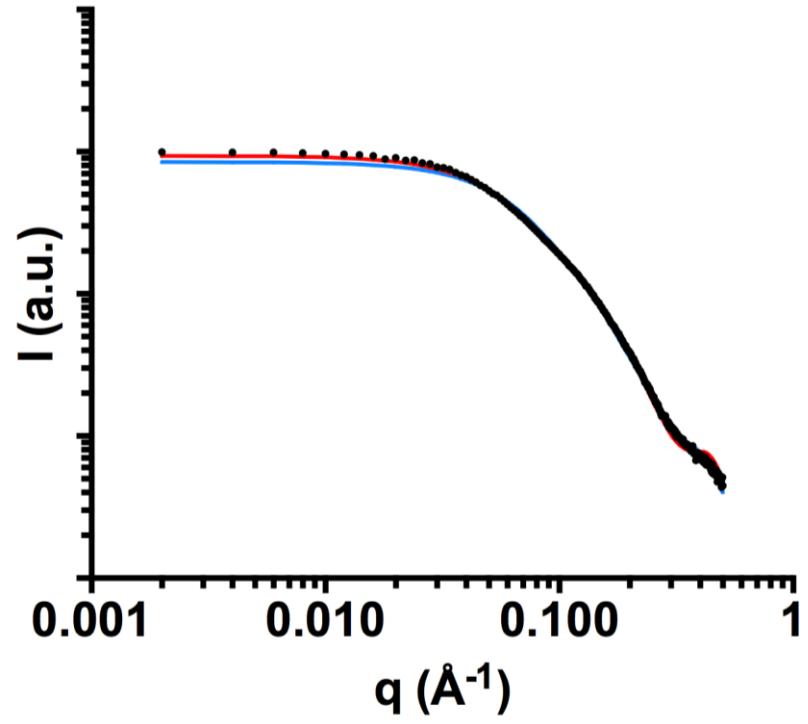

B

Fig. S4

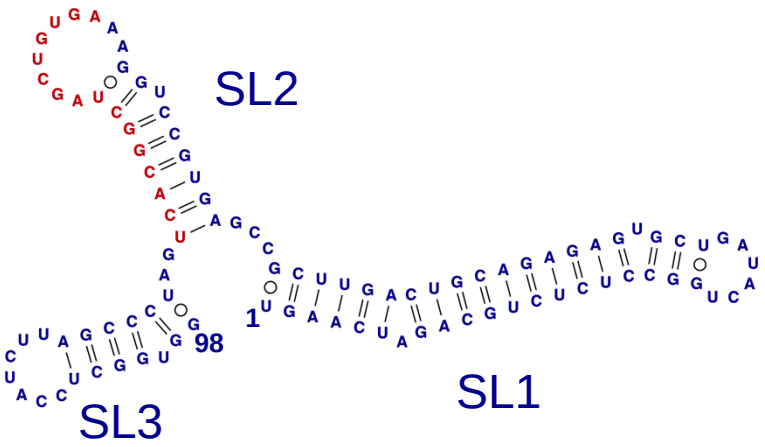

A

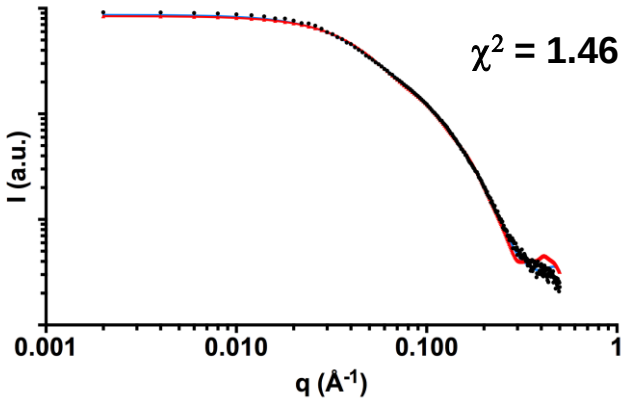

B

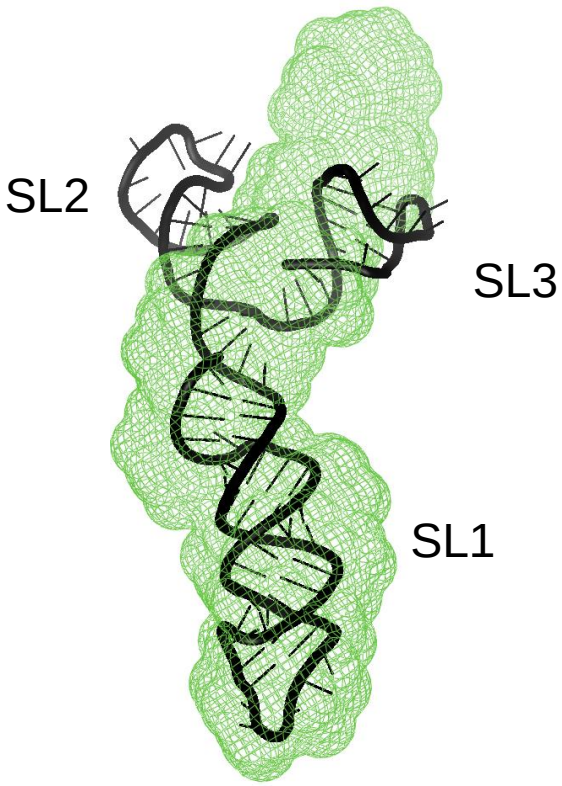

C

Fig. S5

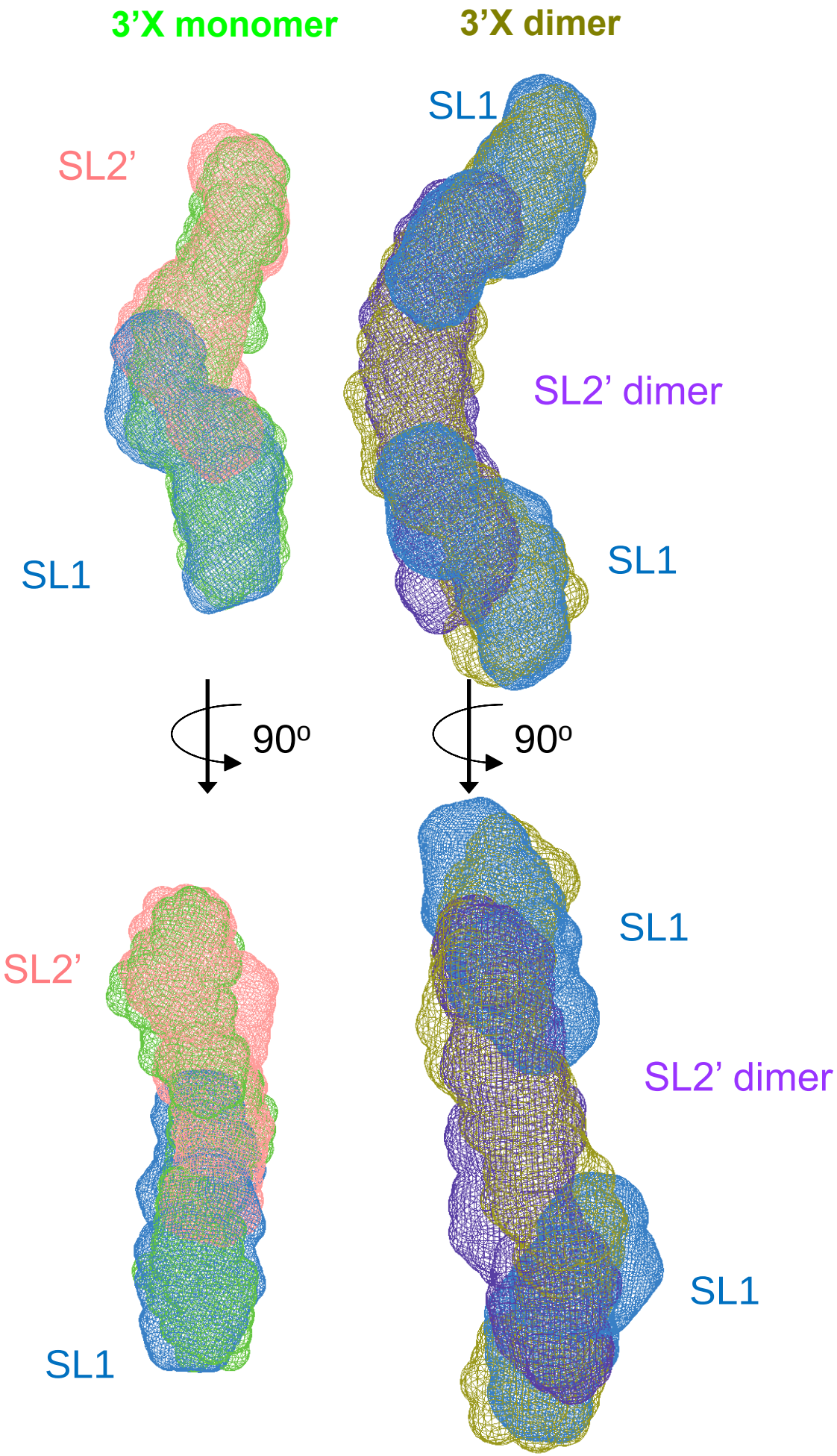
3'X monomer
3'X dimer
SL2'
SL1
SL1
SL2' dimer
SL1
90º
90º
SL2'
SL1
SL1
SL2' dimer
SL1
A
B

Fig. S6